WARSAW UNIVERSITY OF TECHNOLOGY Index 351733
FACULTY OF CIVIL ENGINEERING
COMMITTEE FOR CIVIL AND WATER ENGINEERING
POLISH ACADEMY OF SCIENCES ISSN 1230-2945

DOI: 10.24425/ace.2025.156166

ARCHIVES OF CIVIL ENGINEERING

Vol. LXXI ISSUE 4 2025

pp. 219 –237

Research paper

Application of General Method for tapered built-up CFS C-members – experimental verification

Marcin Górski[1], Katarzyna Sieńkowska-Szpetnar[2], Rafał Budziński[3]

Abstract: An experimental study of tapered built-up cold-formed channel sections was conducted by the authors and described in this paper. The test plan involved testing specimens of varying geometries in bending, compression or eccentric compression cases. The investigation concerned the influence of parameters such as the slenderness of section parts, the difference in section height, and the spacing of intermediate plates on the resistance of the members and possible buckling failure modes. Although most of the analysed sections were classified as Class 4, i.e., susceptible to local and distortional instabilities, global forms were mainly observed. The maximum experimental load values were then used to verify the accuracy in determining the overall resistance of the considered members using the General Method with some "engineering" simplifications. The comparison shows that General Method with implemented assumptions provide a safe estimate of the resistance in the vast majority of cases and in this form can be used to calculate this type of members.

Keywords: cold-formed elements, tapered members, General Method, experimental tests

[1]PhD., Eng., Rzeszów University of Technology, Faculty of Civil and Environmental Engineering and Architecture, Powstancow Warszawy 12, 35-859 Rzeszow, Poland, e-mail: m.gorski@prz.edu.pl, ORCID: 0000-0002-9338-4247
[2]MSc, Eng., Rzeszów University of Technology, Faculty of Civil and Environmental Engineering and Architecture, Powstancow Warszawy 12, 35-859 Rzeszow, Poland, e-mail: k.sienkowska@prz.edu.pl, ORCID: 0000-0003-1497-5821
[3]MSc., Eng., Rzeszów University of Technology, Faculty of Civil and Environmental Engineering and Architecture, Powstancow Warszawy 12, 35-859 Rzeszow, Poland, e-mail: r.budzinski@prz.edu.pl, ORCID: 0000-0002-9890-845X

1. Introduction

At present, cold-formed steel (CFS) sections have become a competitive alternative to hot-rolled members in single-story industrial buildings consisting of repetitive portal frames. These structures are designed primarily with built-up members with two CFS sections in the 'back to back' position. Such cross sections are vertically symmetrical, so that loads are transmitted at the shear centre and do not cause torsion. Moreover, these solutions allow structural joints to be easily formed [1, 2].

The variety of CFS sections refers not only to the shape of the cross section but also the number and location of longitudinal stiffeners. They aim to limit the influence of local forms of buckling of slender parts, thus the material is utilized in the most efficient way [1, 3]. The negative effects of these instabilities are captured in the calculations of the effective cross-sectional characteristics [4].

Current research trends in CFS structural members are largely concerned with non-standard cross-sectional solutions. Wan & Mahendran [5], Steaua et al. [6] and Pawlak & Paczos [7] studied the concept of hollow flange channel sections. Meza et al. [8, 9] and Wang & Young [10] tested a wide range of various built-up members composed of channel sections. Joó et al. [11] and Nuttayasakul et al. [12] analysed quasi-hollow sections consisting of two channels.

The aforementioned solutions for built-up members are mostly based on the shape of I-sections or hollow sections, which refer to standard hot-rolled products. Concepts based on references to conventional steel members may not be limited to transverse shaping. For example, a variation of the section height, creating a tapered shape of the member, may also prove beneficial in certain structures [13]. Studies on tapered thin-walled members usually refer to welded I-sections with slender parts. Experimental testing of such members was carried out by Tankova et al. [14] and Ibrahim et al. [15]. A numerical approach to this problem was described by Jin et al. [16]. Theoretical formulations on buckling of these sections were developed by Asgarian et al. [17] and Osmani & Meftah [18]. There is a lack of publications on thin-walled tapered members in mixed loading cases, especially with built-up cross section consisting of two C- or Z-sections, commonly used in CFS portal frames.

The resistance of rafters and columns in portal frames, which are commonly designed as tapered members, is mainly affected by global forms of buckling. The base cases are the flexural, torsional or flexural-torsional buckling in pure compression and the lateral-torsional buckling in pure bending. However, because of the simultaneous occurrence of bending and compression, the loss of stability of these members takes mixed forms of buckling. The consideration of this type of global instability is possible using the finite element method (FEM) with geometrical nonlinear analysis with imperfections (GNIA), optionally with consideration of material nonlinearities (GMNIA). In addition, the numerical model should consist of at least shell elements [19]. Such analysis requires advanced FEM tools, as well as knowledge and experience of the designer. For this reason, simplified "engineering" procedures for calculating the stability of elements are desirable. EN 1993-1-1 [20] provides two direct methods for predicting the buckling resistance for mixed load cases. An algorithm featured in Section 6.3.3

of the standard called the "Interaction method" gives formulas (6.61) and (6.62), but they cover only single uniform members. The procedure called the "General Method", presented in Section 6.3.4 of the standard, considers a wider range of cases, including, among others, also the tapered and monosymmetric members. An alternative to the aforementioned methods is the use of the "Overall imperfection method" included in Section 5.3.2 of the standard. The general formula behind this procedure uses local and global imperfections in elastic buckling forms. However, the application of this approach for the stability calculations is not easy as it requires certain assumptions and further elaboration. The presented methods were compared and evaluated in view of the safety assessment for a range of uniform hot-rolled members by Hajdu & Papp [21].

In this article, the authors present results of an original study on built-up CFS tapered members with different geometry variations, subjected to compression, bending and the interaction of these cases. The concept of tapered sections was adopted following the idea of effective material utilisation, which is one of the main topics in the field of CFS structures. The selected loading cases combined with certain support conditions were intended to simulate the performance of portal frame members, in which the variation of the section height is used. The basic purpose of this study was the validation of numerical models for further FEM analysis, which will be held in future papers. In this paper, the results of the experimental study were used to evaluate the applicability of the General Method as a most engineering-friendly procedure for preliminary estimation of the resistance of these members using available engineering tools and certain simplifying assumptions.

2. General method for buckling of structural components

The General Method is the adaptation of the Overall Method which was initially introduced by Mueller in [22]. It uses a Merchant-Rankine type of empirical interaction expression which allows one to calculate separately the in-plane and out-of-plane effects. This approach simplified the task because linear buckling analysis (LBA) is sufficient to achieve satisfactory results. The General Method algorithm also includes the reduction factors, making the calculation process comparable to the commonly used Interaction Method in some steps.

According to General Method, overall resistance to out-of-plane buckling of the structural component is ensured if:

$$\frac{\chi_{op}\alpha_{ult,k}}{\gamma_{M1}} \geq 1{,}0 \tag{2.1}$$

where: $\alpha_{ult,k}$ – the minimum load amplifier of the design loads to reach the characteristic resistance of the critical cross section of the structural component considering only in-plane behaviour. This factor should include all relevant in-plane effects, such as geometrical deformation and imperfections, χ_{op} – the reduction factor depended on the slenderness $\overline{\lambda}_{op}$ taking into account the out-of-plane behaviour of the structural component.

The slenderness is non-dimensional value and it should be determined from:

$$\overline{\lambda}_{op} = \sqrt{\frac{\alpha_{ult,k}}{\alpha_{cr,op}}} \tag{2.2}$$

where: $\alpha_{cr,op}$ – the elastic critical load factor for out-of-plane stability of the structural component, without accounting for in-plane flexural buckling.

The standard [20] gives two methods to determine the reduction factor χ_{op}:

a) as the minimum value of χ for lateral buckling and χ_{LT} for lateral torsional buckling,
b) as the interpolated value between the above factors.

Several research papers dealt with the accuracy of General Method in various applications. Da Silva et al. [23] have proven that General Method gives the safety assessment of resistance for prismatic hot-rolled members in case of the interaction of bending and compression. Hajdu & Papp [24] confirmed that conclusion on the 790 different simulations. Czepiżak [25] and Bijlaard et al. [26] proposed their own modifications of the method to improve computational efficiency or compliance. Szalai and Papp [27] indicated a fine accuracy of General Method in case of welded tapered members. Papp et al. [28] used General Method to analyse the single asymmetrical cold-formed section. The results of studies presented in this paper allows to expand the applicability of General Method to tapered cold formed built-up elements.

3. Scope of the study

The research concerned load-bearing elements of single-storey industrial buildings, i.e. frame columns and rafters subjected to bending and compression. The scope of the study covered tapered two-chord elements, consisting of two channels in a 'back-to-back' position (see Fig. 1). The study concerned the influence of parameters such as the slenderness of the section parts, the difference in section height at both ends and the spacing of intermediate plates on the resistance of the members and possible buckling failure modes. The number of values within each variable has been limited to 3 such that are most likely to influence the results of the study. Fixed values were set for the following geometry parameters: element length of 5 m, height of the cross section at the lower of 200 mm, flange width of 80 mm, single edge fold stiffeners of 30 mm and thickness of the intermediate plate of 10 mm. The variation ranges of the parameters were chosen so that both global (stocky sections) and local and distortional buckling (slender sections) would occur. On this basis, the following parameter values were adopted: plate thickness t of 2, 4 or 6 mm; height of the specimen at the wider end h_1 of 300, 500 or 700 mm; number of intermediate plates along the length of the element n of 2, 4 or 6 pcs. The samples were subjected to three types of load:

– pure bending (M),
– pure compression (N),
– combination of bending and compression ($M + N$) with eccentricity $e = \frac{M}{N} \approx 1{,}0$ m.

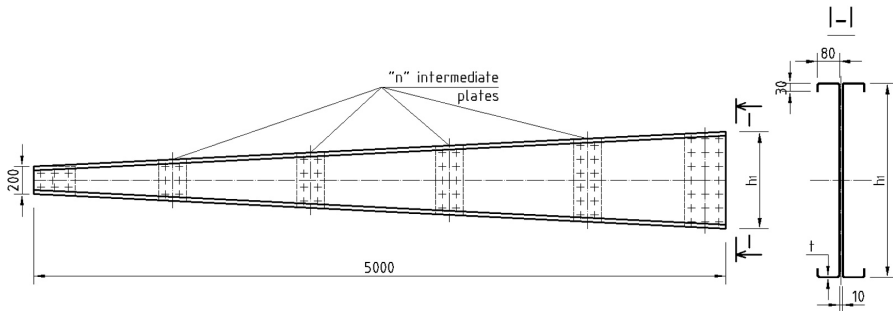

Fig. 1. Schematic side view and cross section of the tested sample

The selection of the specimen parameters was performed based on Hartley's PS/DS.-P:Ha4 poliselective experimental plan based on the Latin hypercube [29]. A summary of the variable parameters of the samples is given in Table 1. Additionally, a test of four samples (S18-S21) outside the adopted plan was performed.

Table 1. Summary of the test sample parameters according to Hartley's poliselective plan of experiment PS/DS.-P:Ha4.

Sample symbol	**Values of input variables**			
	t **[mm]**	h_1 **[mm]**	n **[pcs.]**	**Load type**
S1	6	300	2	N
S2	2	700	2	N
S3	2	300	6	N
S4	6	700	6	N
S5	6	300	2	M
S6	2	700	2	M
S7	2	300	6	M
S8	6	700	6	M
S9	2	500	4	$M + N$
S10	6	500	4	$M + N$
S11	4	300	4	$M + N$
S12	4	700	4	$M + N$
S13	4	500	2	$M + N$
S14	4	500	6	$M + N$
S15	4	500	4	N
S16	4	500	4	M
S17	4	500	4	$M + N$
S18	4	500	2	M
S19	3	700	4	M
S20	6	700	4	M
S21	6	700	4	N

The majority of specimens from the presented plan are classified as class 4 cross sections, which means that they are prone to the effects of local instabilities. However, in some cases the classification was close to the boundary between classes 3 and 4. A few examples of webs of class 3 and higher were obtained for the bending case. Therefore, forms of failure are expected to be associated with global buckling for specimens with relatively robust parts (e.g., S1, S8, S10), mixed buckling cases for sections with average slenderness ratios (e.g., S11, S12, S17), and local and distortional instabilities for members with the most slender parts (e.g. S2, S7, S9).

The investigation was focused on obtaining experimental buckling failure resistances for a wide range of parameters in order to extract and verify normative tools to reliably estimate these values for the studied case of tapered CFS members. The analysis according to the Hartley's plan approach, from which the presented number and variation of specimens is derived, is planned to be complemented by numerical model results and set as the subject of a separate study.

4. Test setup, instrumentation and loading sequence

The test standing had universal character and allowed to test all of the samples mentioned in Section 3, including those subjected to a combined bending moment and axial compression force. The static schema of the members assumed a hinged fork support on the one end (with a minor cross-section height) and a fixed joint with an additional element on the other end (with a major cross-section height). The additional element was supported by a pin connection located at the point of intersection of the member axes and this element. It was used to input an eccentricity of the applied force, which caused a bending moment in the member. Depending on the loading schema, the load was applied by one or two horizontally located Instron Schenck 630 kN. The first was situated in the line of the member axis and was generating the axial compression force, while the second was situated in a distance 1.6 m above the axis of the member and was generating a bending moment (Fig. 2). The actuators were steered by controlling the displacements of their pistons with simultaneous consideration of the actual force in each actuator. Before the essential test, the force with a value of 10 kN was applied by the respective actuator on the member for 1 minute. The purpose of such an operation was to initial align the samples in the test standing. In the case of pure compression or pure bending, the load was applied with constant displacement rate of the piston and the resistance of the members was determined on the basis of the highest force values achieved in the respective actuator. For cases with combined bending moment and axial compression force, the load was applied by both actuators alternately in small steps to achieve an approximately constant ratio between forces in each actuator. The simultaneous decrease of the forces in both actuators was considered as achieving the resistance of the members.

(a)

(b)

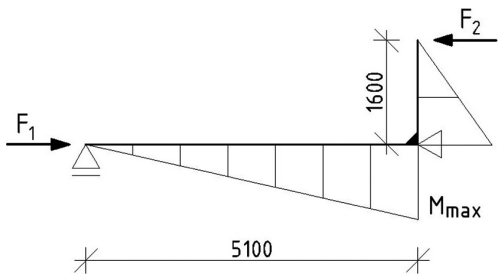

Fig. 2. (a) View of the test standing and (b) static schema with a bending moment diagram

In addition to the forces in the actuators and the displacements of their pistons, the displacements of selected points of the one chord of built-up member were measured during the tests, using LVDT inductive displacement sensors. The number and arrangement of the sensors depended on the geometry of the tested member, especially the number of packing plates, and varied between 14 and 18 sensors. Four sensors measuring vertical displacement of the bottom flange were used. They were situated at a distance of ¼, ½ and ¾ span from the fixed end (named respectively: V1, V2 and V3). The additional, fourth sensor (V4) was located at the point of the highest expected vertical displacement derived from static analysis. Sensors measuring the horizontal displacement of the top flange (HF) and the centre of the web (HW) were placed in cross sections halfway between each of the packing plates. In the case of sample with only two packing plates, additional horizontal displacements of cross sections located at distance ¼ and ¾ between the internal packing plates were also measured. The numbering of cross sections was chosen so that the cross-section situated in the middle of the member always had the number 4. The arrangement of the displacement sensors is shown in Fig. 3.

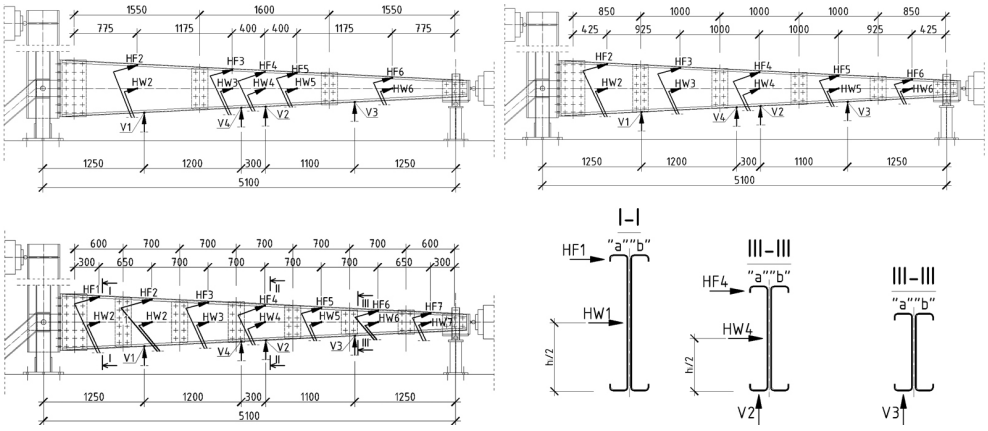

Fig. 3. Arrangement of the LVDT inductive displacement sensors for each type of members tested

Furthermore, one sample (S-18) was equipped with foil strain gauges placed on the opposite chord to measure the strain in the longitudinal direction of the member. The strain gauges were placed on the top flange (TF1 – TF8), the bottom flange (BF4 and BF8) and in the centre of the web of the member (W2 and W6) as shown in Fig. 4.

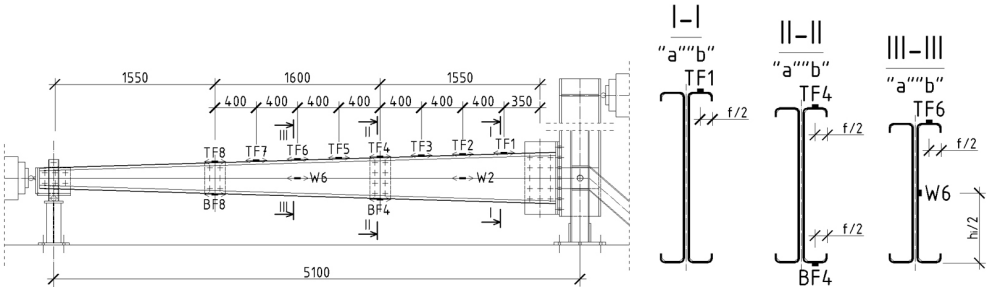

Fig. 4. Arrangement of foil strain gauges in sample S18

5. Results of experimental tests

The material properties of the steel were derived from experimental tests of the pieces obtained from the insignificantly loaded parts of the section samples. The experimental stress-strain curves for each thickness group are presented in Figure 5. The mean values of the yield strength and tensile strength of the steel tested for each thickness group are summarised in Table 2. The maximum values of the carried loading and failure modes of the tested members are presented in Table 3. Some of the samples subjected to axial compression did not fail at the maximum possible load on the actuator. To achieve the failure of these samples, an additional bending moment from the second actuator was applied.

Various failure modes were identified during the tests. However, some conclusions may already be drawn by comparing maximum experimental values with analytical predictions. The maximum forces transferred by each tested member are mostly lower than the cross-section resistances based on effective geometric properties. This indicates that global forms of instability did have a dominant effect on the resistance of the members under study.

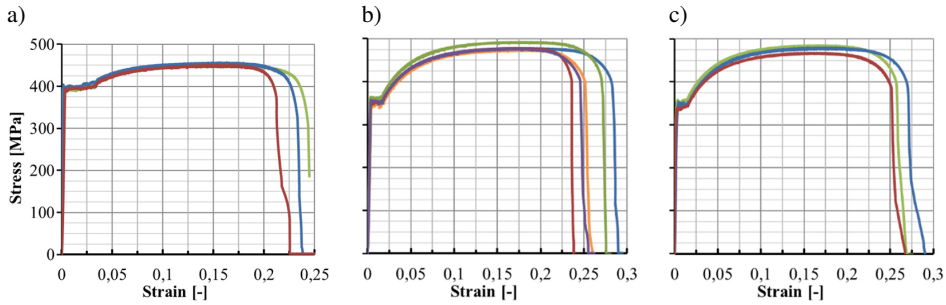

Fig. 5. Stress-strain curves from coupon tests for: (a) 2 mm, (b) 4 mm, and (c) 6 mm thickness group.

Table 2. Mechanical properties of the tested steel

Thickness of test piece [mm]	**Number of specimens [–]**	**Mean value of lower yield strength $R_{eL,mean}$ [MPa]**	**Mean value of tensile strength $R_{m,mean}$ [MPa]**
2	3	390	452
4	5	382	480
6	3	376	477

Table 3. Maximum compression force (F1), maximum bending moment (F2 × r) and failure mode from experimental tests.

Sample symbol	**Maximum compression force (F1)**	**Maximum bending moment (F2×r)**	**Failure mode**
[–]	[kN]	[kNm]	[–]
S1*	446.84	37.18	Elastic flexural buckling of member
S2	234.47	–	Flexural buckling and yield line mechanism in top flange in span
S3	242.54	–	Flexural buckling and yield line mechanism in top flange in span

Table 3 continued at the next page

Table 3 continued from the previous page

Sample symbol	**Maximum compression force (F1)**	**Maximum bending moment (F2×r)**	**Failure mode**
[–]	[kN]	[kNm]	[–]
S4*	457.82	163.44	Elastic lateral-torsional buckling
S5	–	174.87	Elastic lateral-torsional buckling
S6	–	110.22	Yield line mechanism near fixed end
S7	–	44.62	Yield line mechanism near fixed end
S8	–	384.3	Elastic lateral-torsional buckling
S9	51.2	58.82	Yield line mechanism near fixed end
S10	215.87	206.56	Elastic lateral-torsional buckling
S11	65.05	88.62	Combination of lateral-torsional and distortional buckling
S12	152.99	161.96	Combination of lateral-torsional and distortional buckling
S13	115.56	144.47	Lateral-torsional buckling and yield line mechanism in top flange in span
S14	125.97	130.27	Elastic lateral-torsional buckling
S15*	433.78	35.56	Flexural buckling and yield line mechanism in top flange in span
S16	–	207.23	Combination of lateral-torsional and distortional buckling
S17	95.47	129.29	Elastic lateral-torsional buckling
S18	–	140.13	Elastic lateral-torsional buckling
S19	–	145.91	Lateral-torsional buckling and yield line mechanism in top flange in span
S20	47.66	286.81	Elastic lateral-torsional buckling
S21*	572.67	47.84	Elastic flexural buckling

*An additional bending moment was applied to achieve the failure of these samples.

According to the assumptions of the testing plan, various buckling forms were expected depending on the slenderness of the cross-section parts. Ultimately, in the experimental testing, the majority of the samples failed due to global instabilities. In these cases, lateral torsional and flexural buckling were observed in the members in compression and bending, respectively.

An example of lateral torsional buckling leading to a plastic deformation in mid-span of the member S13 is presented in Fig. 6a. Some of the samples with section parts of the lowest wall slenderness ratio presented elastic forms of global instability. Such cases in forms of flexural and lateral torsional buckling for members S1 and S8 are shown Fig. 6b and 6c, respectively. There were also several specimens that failed due to mixed forms of buckling, which combined features of local, distortional or global instabilities. Examples of these cases presented in Fig. 6d and 6e include flexural buckling and yield line mechanism in the top flange of the S3 sample and lateral-torsional instability coupled with distortional buckling in the S16 sample, respectively. As expected, members with parts of the highest slenderness ratio presented failure resulting from local buckling of webs and flanges in compression. Fig. 6f shows an exemplary S6 sample with yield line mechanism occurring due to the local instability in the top flange.

Thanks to the application of horizontally orientated LVDT inductive displacement sensors spaced in the longitudinal direction, it was possible to capture the deflection of the buckling curves along the top flange and web of the specimens. The approximate shapes created from these measures obtained at maximum loading are presented separately for each load case in Figures 7–9. Generally, the deflections of the flange were greater than the corresponding values for the web within the same member. The differences were significant in specimens under bending, which failed due to lateral torsional buckling. The greatest deflections were observed in members with robust parts (low slenderness ratio), especially in compression or mixed loading cases (e.g. S1, S4, S10). These large sags were measured with elastic forms of global instability, which occurred due to significant stiffness of cross-section parts. Asymmetrical, shallow curves were obtained for specimens with high slenderness ratios (eg, S2, S3, S9). In these cases, resistance was influenced by loss of stability within parts of the section, making the global deformations irregular and of smaller magnitude. It shall be noted that only one specimen deflected in an opposite direction with respect to all other samples. This indicates the occurrence of a certain initial eccentricity of the force in the testing stand.

Lastly, no impact of the number of intermediate plates was found on the shape of global forms of buckling. However, this parameter affected the deformations associated with local and distortional instabilities, where the inflections of the curves were shaped within the plates (see Fig. 6e and 6f).

(a)

(b)

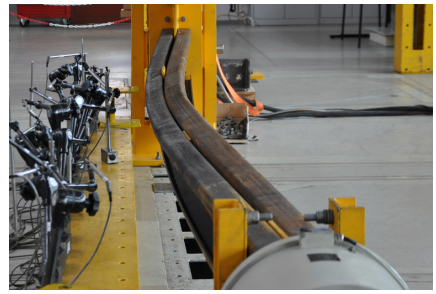

Figure 6 continued on the next page

Figure 6 continued from the previous page

(c) (d)

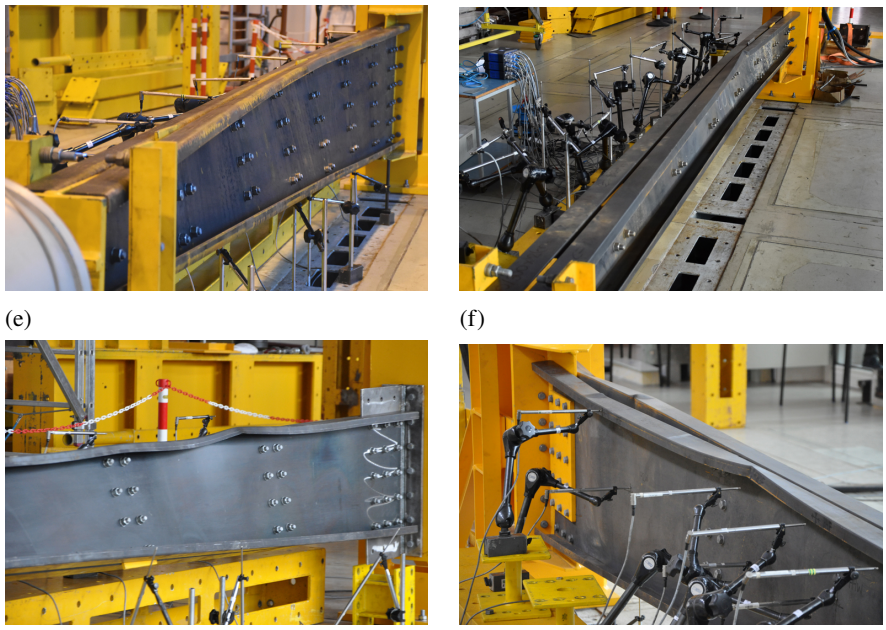

(e) (f)

Fig. 6. Examples of failure modes of the tested specimens (description in the text)

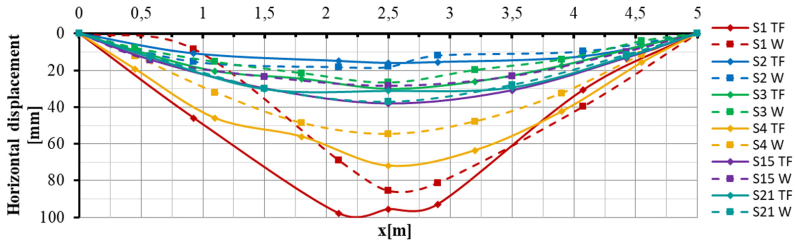

Fig. 7. Top flange (TF) and mid-height web (W) deformations in samples in compression at maximum load

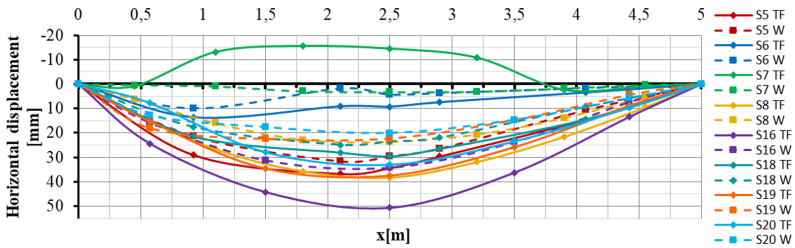

Fig. 8. Top flange (TF) and mid-height web (W) deformations in samples in bending at maximum load

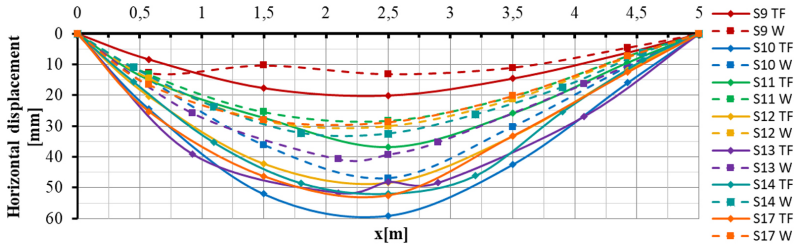

Fig. 9. Top flange (TF) and mid-height web (W) deformations in samples under bending and axial compression at maximum load

Based on the strain measurements for the selected S18 specimen, elastic stresses were determined for different loading levels. These values are plotted as a function of position along the length of the member in Figure 11 in the following section, together with the analytically calculated values.

6. Calculatons using the general method

The resistance of the members was also computed using the General Method. The in-plane factor $\alpha_{ult,k}$ was calculated by formula (6.1) including the global in-plane imperfection and 2^{nd} order effects:

$$\frac{1}{\alpha_{ult,k}} = \frac{N_{Ed}}{N_{Rk,crit}} + \frac{M_{y,Ed,crit} + N_{Ed} \cdot e_{crit} \cdot \left(\frac{1}{1 - \frac{1}{\alpha_{cr,op}}}\right)}{M_{y,Rk,crit}} \tag{6.1}$$

where: N_{Ed} – the design value of the compression force in the critical cross section, $N_{Rk,crit}$ – the characteristic value of the resistance of the critical cross section for uniform compression, $M_{y,Ed,crit}$ – the design value of the bending moment in critical cross section, $M_{y,Rk,crit}$ – the characteristic value of the resistance of the critical cross section for the maximum compressive stress if subject only to moment about the y–y axis, e_{crit} – the value of the initial imperfection in the critical cross section of the element.

Due to class 4 cross sections, the tapered shape of elements and the variable shape of the bending moment diagram, the search for the critical cross section was limited to 11 sections resulting from the division of the element into 10 equal parts every 0.5 m. (see Fig. 10).

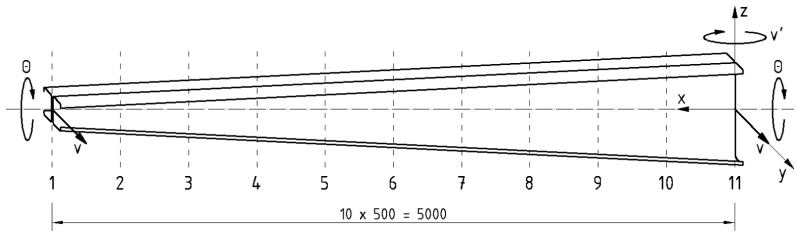

Fig. 10. Cross sections considered in the search for critical stresses and representation of fixed directions at each end of the member applied in LTBeamN

For each cross section, the effective values of the resistance for pure bending and uniform compression due to local and distortional instabilities have been determined according to [4]. In addition, the initial in-plane imperfection of the considered cross sections was calculated as follows:

$$e_i = \frac{L}{300} \cdot \sin\left(\frac{\pi x}{L}\right) \tag{6.2}$$

The calculations were performed using the material parameters presented in Table 1.

Figure 11 shows a comparison of the experimental and computational stress distribution in the top flange of the S18 sample. Until the buckling form appeared, fine agreement between the values was found.

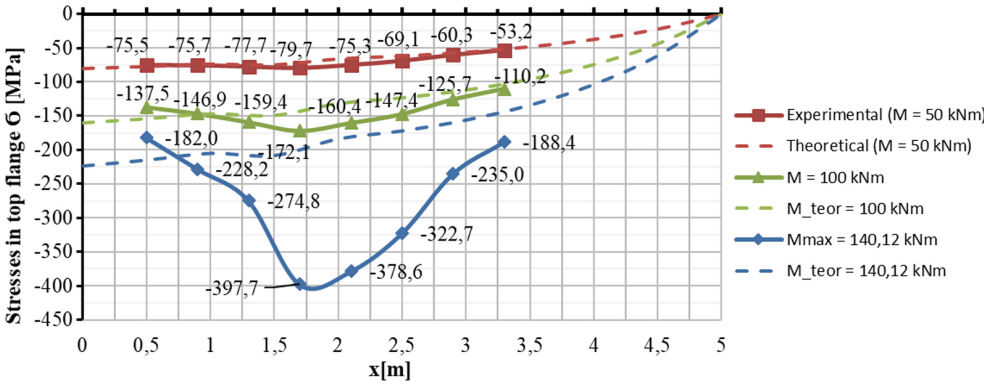

Fig. 11. Stresses in the top flange of S 18 sample from experimental tests (Exp.) and calculations (Calc.) for selected values of bending moment

The out-of-plane factor $\alpha_{cr,op}$ was determined using LTBeamN software. The following boundary conditions were assumed (see Fig. 10):

- at the higher end, 3 directions have been fixed: the lateral displacement of the shear centre of the section (v), the torsion of the section relative to the shear centre (θ) and the rotation of a beam relative to the minor axis of the section (v'),
- at the lower end the lateral displacement of the shear centre of the section (v) and the torsion of the section relative to the shear centre (θ) have been fixed.

The geometry of the tapered built-up C-members has been simplified to the single tapered I – beam cross section with thicknesses of each part equal to the corresponding ones. According to [4], buckling curve "b" for out-of-plane behaviour was used. Table 4 shows the results of the calculations. Furthermore, the utilisation factor was provided, which represents the agreement between experimental and computational results. The utilisation factor was also shown in the bar graph in Fig. 12. Values above 1.0 mean that the experimental values of the internal forces were greater than the calculated resistance, which indicates that the general method gives results on the safe side.

Table 4. Results of buckling calculations using the General Method compared to the experimental results.

Sample symbol	**Critical cross-section**	**Exp. compr. force (F1)**	**Exp. bend. moment (F2×r)**	**Eff. area of crit. section A_{eff}**	**Eff. crit. section modulus W_{eff}**	**Min. load amplifier $\alpha_{ult.k}$**	**Crit. load factor $\alpha_{cr,op}$**	**General Method utilization factor UF**
[–]	[–]	[kN]	[kN · m]	[mm^2]	[mm^3]	[–]	[–]	[–]
S1	9	446.84	26.03	4806	432400	2.19	1.78	0.86
S2	5	234.47	0	1028	190200	1.55	1.18	1.27
S3	6	242.54	0	1040	116400	1.45	1.05	1.40
S4	6	457.82	81.72	5098	862000	1.94	1.35	1.08
S5	11	0	174.87	4858	477000	1.03	2.00	1.26
S6	11	0	110.22	994	337200	1.19	1.06	1.51
S7	11	0	44.62	1036	141000	1.27	1.61	1.19
S8	11	0	384.3	5258	1592800	1.56	1.30	1.19
S9	11	51.2	58.82	1018	239600	1.32	1.24	1.32
S10	11	215.87	206.56	5146	1010400	1.53	1.50	1.11
S11	11	65.05	88.62	2810	328600	1.30	1.69	1.14
S12	11	152.99	161.96	2830	897400	1.63	1.22	1.22
S13	11	115.56	144.47	2838	626400	1.41	1.24	1.28
S14	11	125.97	130.27	2838	626400	1.51	1.31	1.20
S15	8	433.78	24.89	2834	471000	1.75	1.18	1.22
S16	11	0	207.23	2838	626400	1.15	1.10	1.49
S17	11	95.47	129.29	2838	626400	1.59	1.41	1.13
S18	11	0	140.13	2838	626400	1.71	1.63	1.01
S19	11	0	145.91	1846	603000	1.55	1.26	1.22
S20	11	47.66	286.81	5258	1592800	1.99	1.64	0.94
S21	5	572.67	19.14	5040	723600	2.46	1.43	0.96

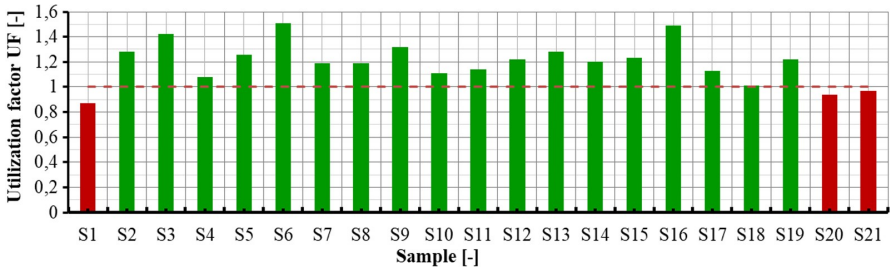

Fig. 12. Values of the utilisation factor for all tested samples according to the General Method

Only 3 of the 21 specimens did not reach the resistance resulting from the calculations according to the General Method. This is due to the fact that significant initial imperfections were observed in these specimens, probably caused by the limitations of the manufacturing process of these sections. These imperfections probably exceeded the values included in the assumed standard buckling curve.

7. Conclusions

In the presented paper, an experimental study of a wide scope of tapered, built up members consisting of two CFS C-sections under bending, compression and eccentric compression was described. The specimens were varied in terms of geometry, resulting primarily in a large range of slenderness ratios of the section parts. Although most of the analysed sections were classified as Class 4, i.e. susceptible to local and distortional instabilities, global forms were mainly observed in the experimental tests. A large influence of global buckling forms was confirmed in the quantitative results, where the maximum experimental forces were mostly lower than the cross sectional resistances calculated from the effective geometric properties. Lastly, the number of intermediate plates, which was another geometric parameter, did not have a significant effect on member resistance or failure modes.

Due to the complex geometry of the tested members, precise determination of their resistance is demanding and time consuming. However, the "engineering" approach presented in this paper, using the General Method with some simplifying assumptions, gives satisfactory results and can be successfully used to estimate the resistance of the tapered built-up cold-formed C-members subjected to axial compression, bending moment, or eccentric compression load. In the vast majority of analysed cases it underestimated the actual resistance determined experimentally and therefore was a safe approach to the analysis of this type of elements. To verify the accuracy of this method, a comparison with results derived from advanced FEM analysis is required.

References

[1] J. Bródka, M. Broniewicz, and M. Giżejowski *Cold-formed sections. Designer's guide*. Rzeszów: Polskie Wydawnictwo Techniczne, 2006 (in Polish).

[2] R. Budziński and L. Ślęczka, "Experimental investigations of steel cold-formed moment-resisting bolted lap joints under monotonic and cyclic loading", *Archives of Civil Engineering*, vol. 69, no. 4, pp. 359–377, 2023, doi: 10.24425/ace.2023.147664.

[3] D. Dubina, V. Ungureanu, and R. Landolfo, *Design of Cold-formed steel structures. Eurocode 3: Design of steel structures. Part 1–3: Design of Cold-formed structures*. Mem Martins, Portugal: ECCS/Wiley-Blackwell/Ernst&Sohn, 2012.

[4] EN 1993-1-3 Eurocode 3 – Design of steel structures – Part 1–3: General rules – Supplementary rules for cold-formed members and sheeting. European Committee for Standardization, 2006.

[5] H.-X. Wan and M. Mahendran, "Structural characteristics of hollow flange channel beams under bending and torsion" in *Proceedings of the 8th International Conference on Advances in steel structures*. Lisbon DECivil/IST/UL, 2015.

[6] E. Steau, P. Keerthan, and M. Mahendran "Web crippling design of hollow flange channel beams under one flange load cases", *ce/papers. Special Issue: Proceedings of Eurosteel 2017*, vol. 1, no. 2–3, 2017, doi: 10.1002/cepa.194.

[7] A.M. Pawlak and P. Paczos, "Analysis of strength and resistance to loss of stability of thin-walled channel columns with non-standard cross-sectional shape", *Archives of Civil Engineering*, vol. 70, no. 3, pp. 101–116, 2024, doi: 10.24425/ace.2024.150973.

[8] F.J. Meza, J. Becque, and I. Hajirasouliha, "Experimental study of cold-formed steel built-up columns", *Thin-Walled Structures*, vol. 149, 2020, doi: 10.1016/j.tws.2019.106291.

[9] F.J. Meza, J. Becque, and I. Hajirasouliha, "Experimental study of the cross-sectional capacity of cold-formed steel built-up columns", *Thin-Walled Structures*, vol. 155, 2020, doi: 10.1016/j.tws.2020.106958.

[10] L. Wang and B. Young, "Behavior of Cold-Formed Steel Built-Up Sections with Intermediate Stiffeners under Bending. I: Tests and Numerical Validation", *Journal of Structural Engineering,* vol. 142, no. 3, 2016, doi: 10.1061/(ASCE)ST.1943-541X.0001428.

[11] A.L. Joó, M. Szedlák, and S. Ádány, "Experimental investigation on double-c compressed members", in *Proceedings of the 8th International Conference on Advances in steel structures*. Lisbon, DECivil/IST/UL, 2015.

[12] N. Nuttayasakul, W. Patwichaichote, and T. Chaisomphob, "Testing of the front to front built-up c-section cold formed steel flexural members using plate and screw connection", in *Proceedings of the 8th International Conference on Advances in steel structures*. Lisbon, DECivil/IST/UL, 2015.

[13] E. Allen and W. Zalewski, *Form and Forces : Designing Efficient, Expressive Structures*. Hoboken: John Wiley & Sons, 2010.

[14] T. Tankova, J.P. Martins, L.S. da Silva, L. Marques, H.D. Craveiro, and A. Santiago, "Experimental lateral-torsional buckling behaviour of web tapered I-section steel beams", *Engineering Structures*, vol. 168, pp. 355–370, 2018, doi: 10.1016/j.engstruct.2018.04.084.

[15] M.M. Ibrahim, I.M. El Aghoury, and S.A.-B. Ibrahim, "Experimental and numerical investigation of ultimate shear strength of unstiffened slender web-tapered steel members", *Thin-Walled Structures*, vol. 148, 2020, doi: 10.1016/j.tws.2020.106601.

[16] S. Jin, Z. Li, S. Xu, and F. Huang, "Constrained shell finite element method for stability analysis of thin-walled steel members with tapered sections", in *Proceedings of the Annual Stability Conference Structural Stability Research Council*. SSRC, 2020.

[17] B. Asgarian, M. Soltani, and F. Mohri, "Lateral-torsional buckling of tapered thin-walled beams with arbitrary cross-sections", *Thin-Walled Structures,* vol. 62, pp. 96–108, 2013, doi: 10.1016/j.tws.2012.06.007.

[18] A. Osmani and S.A. Meftah, "Lateral buckling of tapered thin walled bi-symmetric beams under combined axial and bending loads with shear deformations allowed", *Engineering Structures*, vol. 165, pp. 76–87, 2018, doi: 10.1016/j.engstruct.2018.03.009.

[19] L. Czechowski, M. Kotełko, J. Jankowski, V. Ungureanu, and A. Sanduly, "Strength analysis of eccentrically loaded thin-walled steel lipped C-profile columns", *Archives of Civil Engineering*, vol. 69, no. 3, pp. 301-316, 2023, doi: 10.24425/ace.2023.146082.

[20] EN 1993-1-1 Eurocode 3: Design of steel structures – Part 1-1: General rules and rules for buildings. European Committee for Standardization, 2005.

[21] G. Hajdú and F. Papp, "Safety Assessment of Different Stability Design Rules for Beam-columns", *Structures*, vol. 14, pp. 376-388, 2018, doi: 10.1016/j.istruc.2018.05.002.

[22] C. Müller, "Zum Nachweis ebener Tragwerke aus Stahl gegen seitliches Ausweichen", PhD. thesis, RWTH Aachen, 2003.

[23] L. da Silva, L. Marques, and C. Rebelo, "Numerical validation of the general method in EC3-1-1 for prismatic members", *Journal of Constructional Steel Research*, vol. 66, no. 4, pp. 575–590, 2010, doi: 10.1016/j.jcsr.2009.11.003.

[24] G. Hajdú and F. Papp, "On the accuracy of general method adapted in EN 1993-1-1", *Journal of Constructional Steel Research*, vol. 195, 2022, doi: 10.1016/j.jcsr.2022.107354.

[25] D. Czepiżak, "Innovative Look at the 'General Method' of Assessing Buckling Resistance of Steel Structures", *Studia Geotechnica et Mechanica*, vol. 43, no. 4, pp. 1-9, 2021, doi: 10.2478/sgem-2021-0022.

[26] F. Bijlaard, M. Feldmann, J. Naumes, and G. Sedlacek, "The general method for assessing the out-of-plane stability of structural members and frames and comparison with alternative rules in EN 1993 – Eurocode 3 – Part 1–1", *Steel Construction,* vol. 3, no. 1, pp. 19–33, 2010, doi: 10.1002/stco.201010004.

[27] F. Szalai and J. Papp, "Theory and application of the General Method of Eurocode 3 – Part 1–1", presented at Eurosteel, 31 August – 2 September 2011, Budapest, Hungary, 2011.

[28] F. Papp, A. Rubert, and J. Szalai, "DIN EN 1993-1-1-konforme integrierte Stabilitätsanalysen für 2D/3D-Stahlkonstruktionen (Teil 1)", *Stahlbau*, vol. 83, no. 1 pp. 1–15, 2014, doi: 10.1002/stab.201410128.

[29] Z. Polański, *Planning of experiments in science.* Kraków, Polska: Wydawnictwo Naukowo Techniczne, 1984 (in Polish).

Zastosowanie Metody Ogólnej do obliczeń elementów zbieżnych o przekroju złożonym ze stalowych kształtowników giętych na zimno – weryfikacja doświadczalna

Słowa kluczowe: kształtowniki gięte, elementy zbieżne, Metoda Ogólna, badania doświadczalne

Streszczenie:

W pracy przedstawiono wyniki badań doświadczalnych dwugałęziowych elementów z giętych na zimno ceowników o przekroju zbieżnym w przypadkach czystego zginania, czystego ściskania lub interakcji zginania
i ściskania. Schemat statyczny i sposób obciążania zaprojektowano w nawiązaniu do warunków pracy elementów ram portalowych, które z uwagi na zmienny rozkład momentów zginających kształtuje się o zmiennym przekroju i projektuje na tzw. stałą siłę. Analizę wpływu takich parametrów jak grubość ścianki t (2, 4 lub 6 mm), liczba przewiązek gałęzi n (2, 4 lub 6 sztuk) oraz maksymalna wysokość przekroju zbieżnego h_1 (300, 500 lub 700 mm) na nośność i postać niestateczności elementów przeprowadzono na podstawie 21 zróżnicowanych przypadków doświadczalnych. Pomimo, iż większość próbek sklasyfikowano jako przekroje klasy 4, to dominującą formą niestateczności okazały się być formy globalne lub mieszane, tzn. wykazujące jednocześnie cechy wyboczenia globalnego i dystorsyjnego lub lokalnego. Maksymalne siły uzyskane z badań doświadczalnych okazały się w większości niższe niż nośności przekroju obliczone na podstawie efektywnych charakterystykach geometrycznych przekrojów, uwzględniających wpływ lokalnych i dystorsyjnych form niestateczności. Oznacza to, że globalne formy niestateczności miały dominujący wpływ na nośność badanych elementów.Nośność badanych elementów została określona również obliczeniowo przy użyciu Metody Ogólnej według wytycznych EC3-1-1. Na potrzeby tej analizy przyjęto pewne założenia, mające na celu uproszczenie wybranych kroków obliczeniowych:

– rzeczywisty przekrój złożony z dwóch ceowników zwróconych do siebie plecami zastąpiony litym przekrojem dwuteowym o analogicznej geometrii przy wyznaczeniu współczynnika obciążenia krytycznego $\alpha_{cr,op}$ w programie LTBeam
– wyznaczenie naprężeń krytycznych z wykorzystaniem efektywnych charakterystyk geometrycznych przekrojów, obliczonych wyłącznie dla przypadków czystego ściskania (efektywne pole powierzchni przekroju A_{eff}) i zginania (efektywny wskaźnik wytrzymałości przekrojuW_{eff})

Wyniki obliczeń przedstawiono w formie wskaźników wykorzystania nośności z metody ogólnej, obliczonych dla maksymalnych obciążeń z badań doświadczalnych. Dla zdecydowanej większości przypadków otrzymano wartości powyżej 1,0, co oznacza, że zastosowane podejście prezentuje zadowalające oszacowanie nośności w analizowanym zakresie elementów. Zaprezentowane podejście „inżynierskie", wykorzystujące Metodę Ogólną z pewnymi uproszczeniami, daje zadowalające wyniki i może być z powodzeniem stosowane do szacowania nośności elementów zbieżnych złożonych ze stalowych kształtowników giętych, poddanych ściskaniu osiowemu, momentowi zginającemu lub mimośrodowemu ściskaniu. Jednak aby zweryfikować dokładność tej metody, należy przeprowadzić szerokie porównanie z wynikami uzyskanymi na podstawie zaawansowanej analizy metodą elementów skończonych.

Received: 2025-06-04, Revised: 2025-07-24